Supporting Information

Facile One-pot Polymerization of a Fully Conjugated Donor-acceptor Block Copolymer and its Application to Efficient Single Component Polymer Solar Cells

Chang Geun Park,‡ Su Hong Park,‡ Youngseo Kim,‡ Thanh Luan Nguyen, Han Young Woo, Hungu Kang, Hyo Jae Yoon, Sungnam Park*, Min Ju Cho* and Dong Hoon Choi*

Department of Chemistry, Research Institute for Natural Sciences, Korea University, 145 Anam-Ro, Sungbuk-gu, Seoul 02841 South Korea

‡ These authors contributed equally to this work.

*Corresponding authors: S. Park (spark8@korea.ac.kr), M. J. Cho (chominju@korea.ac.kr), D. H. Choi (dhchoi8803@korea.ac.kr)

Table S1. Research trends of single component-PSCs efficiencies of SC-PSCs using CBP without PT blocks.

Year	Type	PCE (%)	Reference
2006	P3HT free	0.20	S1
2009	P3HT free	1.50	S2
2011	P3HT free	1.75	S3
2014	P3HT free	0.89	S4
2014	P3HT free	2.70	S5
2015	P3HT free	0.54	S6
2016	P3HT free	0.22	S7
2017	P3HT free	1.54	S8
2017	P3HT free	3.87	S9
2019	P3HT free	5.28	In this work

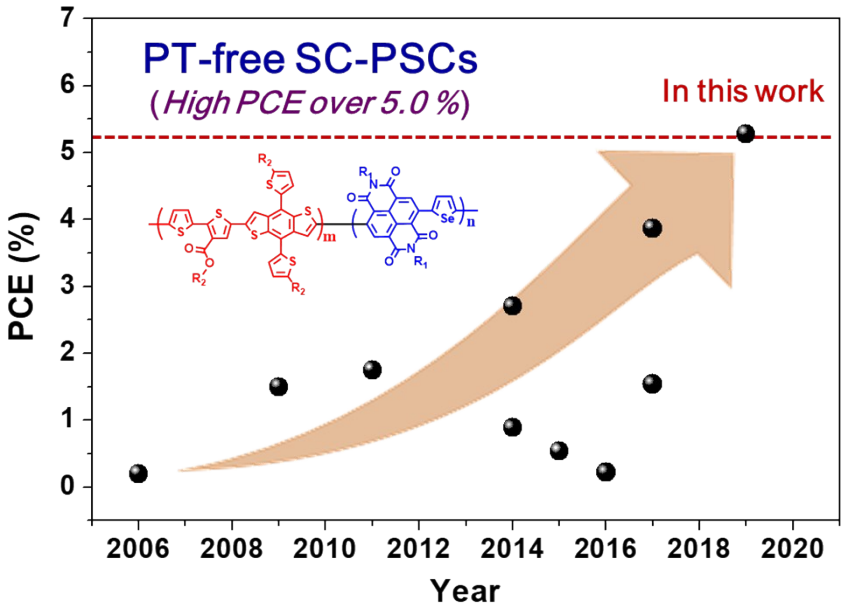

Figure S1. Development trend of PCE value of SC-PSC using CBP without PT blocks.

EXPERIMENTAL SECTION

Materials

All chemicals used for the synthesis of the **CDABP** bearing donor and acceptor blocks via one-pot polymerization were purchased from Sigma-Aldrich, Acros Organics Co., and Tokyo Chemical Industry and used without further purification. The reagent grade solvents used in this experiment were freshly dried *via* the standard distillation methods. Compounds **M1**, **M2,** and **M3** were synthesized according to published methods.[S9]

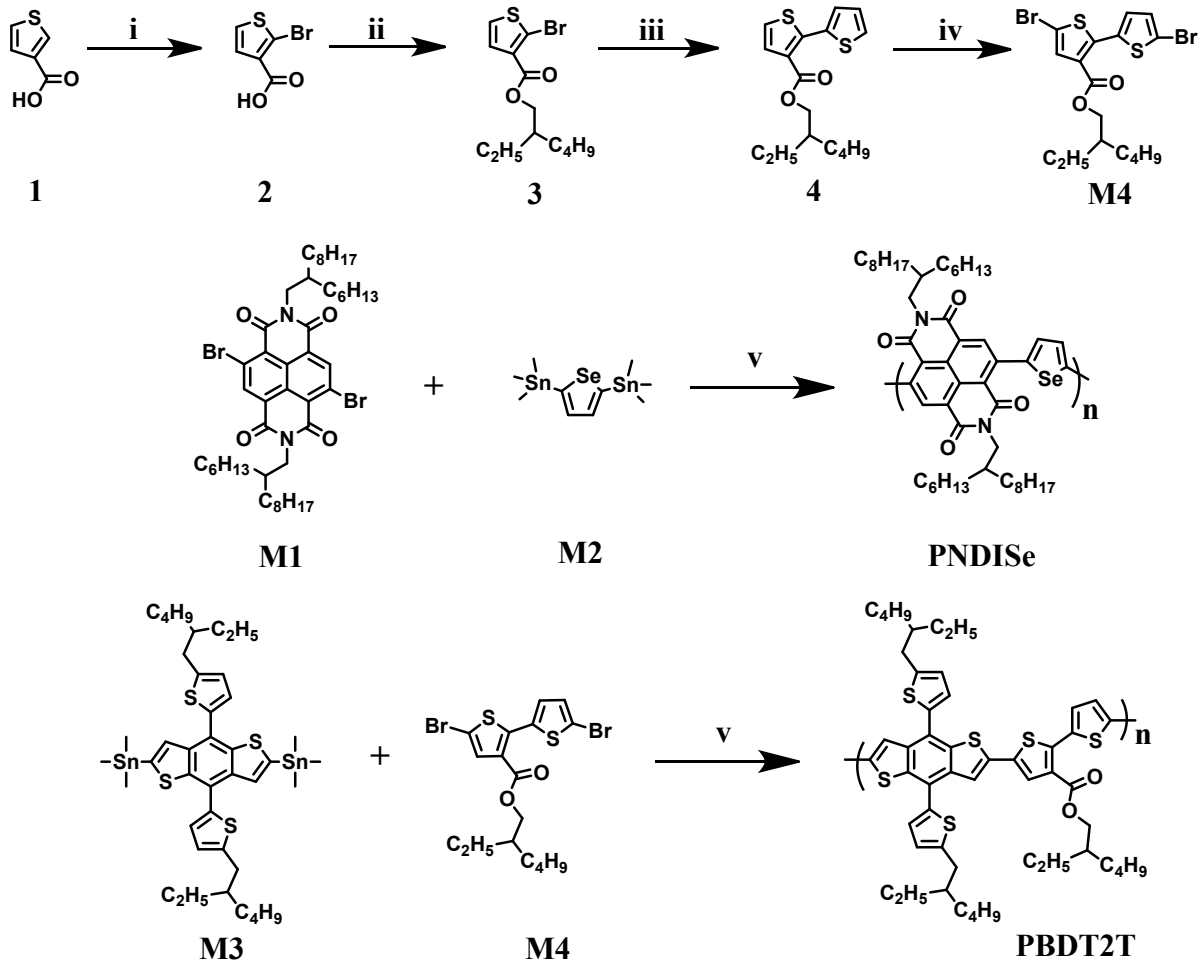

Scheme S1. Synthetic procedure of PNDISe and PBDT2T: i) *n*-BuLi, Br_2, THF; ii) K_2CO_3, 2-Ethylhexyl bromide, DMF; iii) 2-(tributylstannyl)thiophene, P(*o*-tolyl)$_3$, $Pd_2(dba)_3$, toluene; iv) NBS, DMF; v) P(*o*-tolyl)$_3$, $Pd_2(dba)_3$, toluene.

Synthesis

2-Bromothiophene-3-carboxylic acid (2)

Compound **1** (4.00 g, 31.2 mmol) was dissolved in 50 mL of tetrahydrofuran and then the solution was cooled to -78 °C and 2.5 M *n*-butyllithium (25.2 mL, 63.0 mmol) was gradually added dropwise. The reaction mixture was stirred for 30 min at -78 °C and bromine (1.73 mL, 32.8 mmol) was slowly added into the mixture. The reaction was allowed to continue overnight after warming up to 25 ^{o}C. After stirring the mixture overnight, a small amount of 1 M HCl (50.0 mL) was added to quench the reaction. After extracting the resultant mixture using ethyl acetate and water, the organic layer was dried with Na_2SO_4. Compound **2** was recrystallized twice in a H_2O/ethanol mixture to furnish the pure compound as a faint grey solid (5.10 g, yield 78.9%). ^{1}H NMR (500 MHz, DMSO-d_6, δ (ppm)): 13.09 (s, 1H), 7.63−7.62 (d, J = 5.5 Hz, 1H), 7.32−7.31 (d, J = 5.5 Hz, 1H).

2-Ethylhexyl 2-bromothiophene-3-carboxylate (3)

A mixture of compound **2** (2.00 g, 9.66 mmol) and K_2CO_3 (4.00 g, 28.9 mmol) was dissolved in 20 mL of dimethylformamide (DMF). The mixture was stirred for 1 h under argon atmosphere. 2-Ethylhexyl bromide (5.60 g, 28.9 mmol) was added to the mother mixture and stirred overnight. 50 mL of deionized water bearing a small amount of 1 M HCl (2−3 mL) was poured into the mixture to quench the reaction, followed by extraction with CH_2Cl_2. The organic phase was dried with Na_2SO_4 and the solvent was removed in vacuo. The product was purified via silica-gel column chromatography using hexane/CH_2Cl_2 (4:1 v/v), yielding the pure compound as a colorless oil (1.50 g, yield 49.0%). ^{1}H NMR (500 MHz, $CDCl_3$; δ (ppm)): 7.37-7.36 (d, J = 5.5 Hz, 1H), 7.22-7.21 (d, J = 5.5 Hz, 1H), 4.25–4.19 (m, 2H), 1.72–1.67 (m, 1H), 1.50–1.28 (m, 8H), 0.95–0.89 (m, 6H).

2-Ethylhexyl [2,2'-bithiophene]-3-carboxylate (4)

Compound **3** (1.50 g, 4.69 mmol) and 2-(tributylstannyl)thiophene (2.33 g, 7.03 mmol) were dissolved in 20 mL of toluene. The reaction mixture was degassed with argon after adding tris(dibenzylideneacetone)dipalladium ($Pd_2(dba)_3$) (215 mg, 5 mol%) and tri(*o*-tolyl)phosphine (P(*o*-tolyl)$_3$) (285 mg, 20 mol%). The mixture was heated to 110 °C and continuously stirred for 24 h. After the reaction was complete, the mixture was poured into 50 mL of deionized water and then extracted with CH_2Cl_2. The organic phase was dried with Na_2SO_4 and the solvent was removed. The product was purified via silica-gel column chromatography using hexane/CH_2Cl_2 (3:1), yielding the pure compound as a faint yellow oil (1.4 g, yield 92.7%). ^{1}H NMR (500 MHz, $CDCl_3$, δ(ppm)): 7.48−7.47 (d, J = 5.5 Hz, 1H), 7.40−7.38 (m, 2H), 7.20−7.19 (d, J = 5.5 Hz, 1H), 7.07−7.05 (q, J = 5.5 Hz, 1H), 4.17−4.16 (m, 2H), 1.67−1.59 (m, 1H), 1.39–1.25 (m, 8H), 0.95–0.86 (m, 6H).

2-Ethylhexyl 5,5'-dibromo-[2,2'-bithiophene]-3-carboxylate (M4)

Compound **4** (1.40 g, 4.30 mmol) and *N*-bromosuccinimide (NBS) (1.96 g, 10.9 mol) were dissolved in 20 mL of DMF. The mixture was stirred for 24 h at RT. After the reaction was finished, the mixture was poured into 50 mL of deionized water and then extracted with CH_2Cl_2 to remove the acid completely. The product was purified via column chromatography on silica gel using hexane/CH_2Cl_2 (3:1), yielding the pure compound as a yellow oil (1.90 g, yield 89.6%). ^{1}H NMR (500 MHz, $CDCl_3$, δ(ppm)): 7.40 (s, 1H), 7.11−7.10 (d, J = 4.0 Hz, 2H), 7.01−7.00 (d, J = 4.0 Hz, 1H), 7.07−7.05 (q, J = 5.5 Hz, 1H), 4.17−4.10 (m, 2H), 1.63−1.59 (m, 1H), 1.37–1.25 (m, 8H), 0.90–0.84 (m, 6H).

Polymerization of PNDISe

For the PNDISe polymer, **M1** (1 equiv.), **M2** (1 equiv.), $Pd_2(dba)_3$, and P(*o*-tolyl)$_3$ were added to a two-neck round-bottom flask. Dry toluene (8 mL) and anhydrous DMF (2 mL) were then added and the mixture was degassed for 10 min under nitrogen bubbling. The reaction mixture was refluxed for 12 h at 110 °C. After cooling to room temperature (RT), the resulting solution was precipitated into methanol (300 mL). The byproducts, namely the unreacted monomer and oligomers, were removed via the Soxhlet extraction method with acetone, n-hexane, methyl chloride, and chloroform successively. The concentrated chloroform fraction was then precipitated into methanol (300 mL) and dried under vacuum at 60 °C for 24 h. (PNDISe: M_n = 17.8 kDa; PDI = 2.12)

Polymerization of PBDT2T

PBDT2T was synthesized according to PDNISe polymerization. By using the **M3** (1 equiv.), **M4** (1 equiv.), $Pd_2(dba)_3$, and P(*o*-tolyl)$_3$ were added to a 2-neck round bottom flask. Dry toluene (10 mL) was then added and the mixture was degassed. The reactor was stirred and refluxed for 24 h at 110 ^oC. (PBDT2T: M_n = 34.8 kDa, PDI = 3.89)

Instrumentation

The ^1H NMR spectra of all the compounds were analyzed using a Bruker 500 MHz spectrometer (Ascend 500, Bruker). The absorption spectra of the small molecules and polymers in the chloroform solution and thin films were recorded using a UV−vis absorption spectrometer (Agilent 8453, photodiode array, λ = 190−1100 nm). The electrochemical properties were characterized using cyclic voltammetry (CV, eDAQ EA161) with an electrolyte solution comprising tetrabutylammonium hexafluorophosphate (Bu_4NPF_6) in

acetonitrile. A platinum wire and Ag/AgCl were used as the counter and reference electrodes, respectively. The number average molecular weight (M_n) and polydispersity index (PDI) of the polymers were measured relative to polystyrene (PS) standards via gel permeation chromatography (GPC) with 1,2-dichlorobenzene (*o*-DCB) as the eluent using an Agilent GPC 1200 series instrument. The GIWAXD measurements were conducted at the 9A (U-SAXS) beamline (energy = 11.035 keV, pixel size = 79.59 μm, wavelength (λ) = 1.12199 Å, 2θ = 0°−20°) of the Pohang Accelerator Laboratory (PAL). The samples were prepared by spin-coating the polymer solutions onto a SiO_2 wafer.

KPFM measurements were carried out in ambient air, using a Bruker AFM Multimode model in amplitude modulated KPFM. Pt/Ir coated conductive probes (SCM-PIT-V2, spring constant 3 N/m, resonant frequency 75 kHz, Bruker) were calibrated on freshly cut, highly oriented pyrolytic graphite (HOPG) to determine the work function of the tip. Topography and KPFM data were attained simultaneously using a standard two-pass procedure; a topographic line was first acquired in tapping mode and a KPFM line was secondarily acquired in a lift mode. In the lift mode, tip scans were performed at a fixed distance of 80 nm above the active layer surface to ensure dominant electrostatic forces. In KPFM mode, the applied DC voltage has an amplitude of 500 mV at a frequency similar to the resonance frequency of the cantilever. KPFM images of the sample surface were obtained at 0.5 Hz of the probe scan rate with scan size of 5 μm and 512 samples per line over five different regions. We obtained transmission electron microscopy (TEM) imaging using a Tecnai G2F30 transmission electron microscope (FEI Inc., accelerating voltage = 300 kV) to observe the internal morphology of the polymer film.

Space Charge Limited Current (SCLC) Method

To clarify the effect of charge carrier transport ability and their balance on the performance improvement of the SC-PSCs, the hole-only (ITO / PEDOT:PSS / active layers / Au (70 nm)) and electron-only (ITO / ZnO (30 nm) / active layers / LiF (1 nm) / Al (100 nm)) devices were fabricated according to the corresponding SC-PSCs. The *J–V* curves of the hole-only and electron-only devices were measured under dark conditions. The performance of the hole-only device was estimated by measuring the *J-V* characteristics using a Keithley 2400 SourceMeter. The hole mobilities of the PBDT2T were measured via the space charge limited current (SCLC) method. The mobility was calculated according to following equation: $J = 9\varepsilon_0\varepsilon_r\mu V^2/8L^3$, where J is the current density, ε_0 is the permittivity of the HTL, ε_r is the relative dielectric constant, μ is the hole mobility, and L is the thickness of the HTL. The internal voltage, $V = V_{appl} - V_{bi} - V_a$, where V_{appl} is the applied voltage to the device, V_{bi} is related to the work function difference between the two electrodes, and V_a is the voltage drop. [S10]

Fabrication of the SC-PSCs

Inverted solar cells were fabricated with the ITO (150 nm) / ZnO (30 nm) / CDABP (~70 nm) / MoO_3 (10 nm) / Ag (100 nm) configuration. Pre-patterned ITO glass (150 nm, R = 10.0 Ω cm^{-2}) was washed with acetone, deionized water, and isopropyl alcohol for 10 min each in the stated order. A ZnO layer was spin coated on the washed ITO glass at 3000 rpm for 40 s after UV-ozone processing for 20 min and then annealed at 165 °C for 1 h. The substrates were then transferred into a N_2-protected glove box. The CDABP films were obtained by spin coating the chloroform solution (1.0 wt%). The solutions were stirred overnight at 60 °C and spin coated onto an ITO/ZnO substrate at 3000 rpm for 40 s. Then, the as-cast films were

annealed at elevated temperatures (e.g., 120, 140, 160, and 180 °C) for 10 min at ambient conditions. Finally, MoO_3 (10 nm) and Ag (100 nm) were deposited on the photoactive layer by thermal evaporation. The current density−voltage ($J-V$) characteristics were measured using a Keithley 2400 SourceMeter under AM 1.5 G illumination at 100 mW cm^{-2} (Oriel, 1000 W). The incident light intensity was measured using a calibrated broadband optical power meter (Spectra-Physics, Model 404) and the EQE spectra were recorded with a K3100 EQX instrument with a K240 XE300 lamp source.

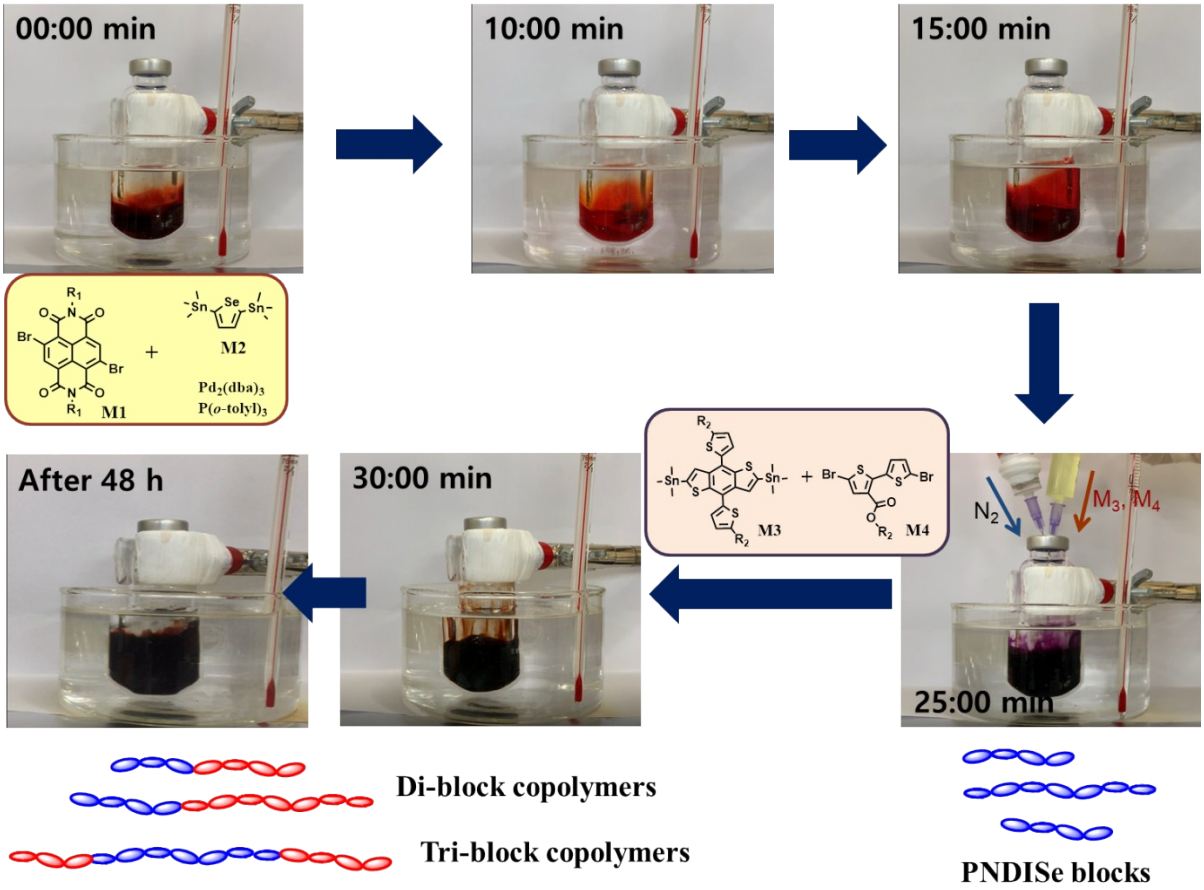

Figure S2. Photographic images showing the progress of one-pot polymerization

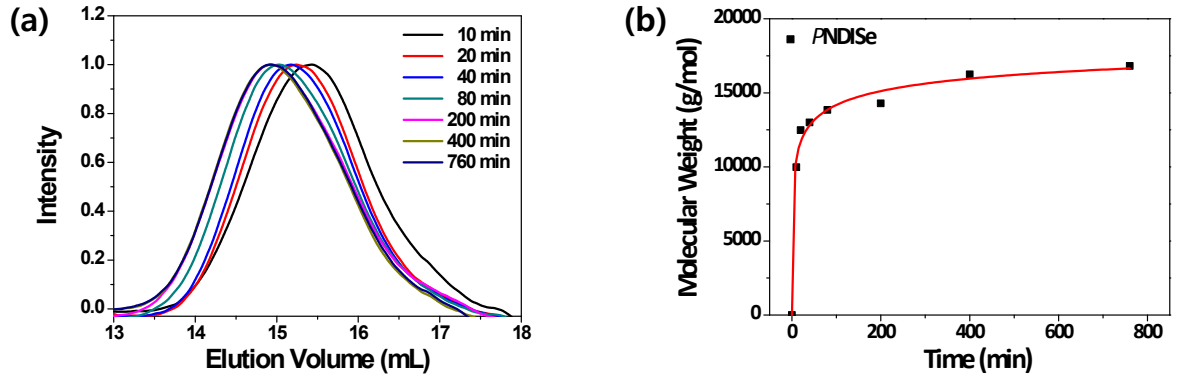

Figure S3. GPC chromatograms of PNDISe block with different time (a) and MW of PNDISe *vs*. polymerization time (b). GPC chromatograms of PNDISe block (polymerization time = 25 min.) and CDABP.

Table S2. MW (M_n) of PNDISe *vs*. polymerization time

Sample	**1**	**2**	**3**	**4**	**5**	**6**	**7**
Time (min)	10	20	40	80	200	400	760
M_n (g/mol)	9972.3	12482	12998	13845	14284	16251	16819
PDI	2.19	2.00	2.06	2.30	2.47	2.23	2.12

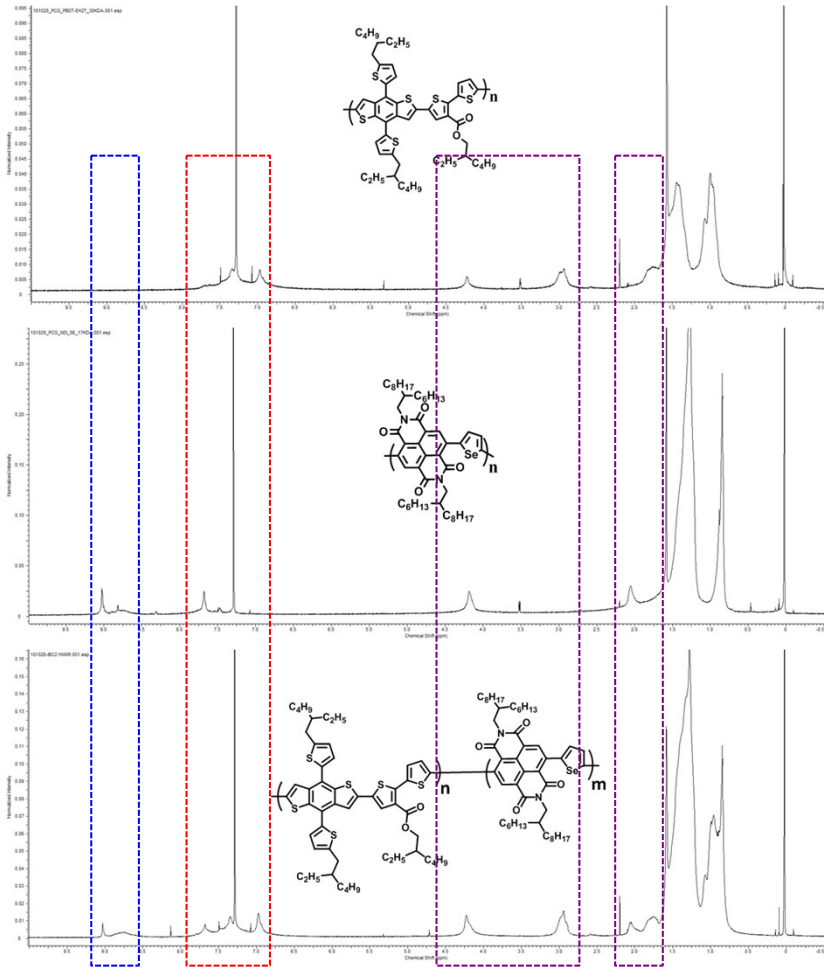

Figure S4. NMR spectra of PBDT2T, PNDISe and CDABP

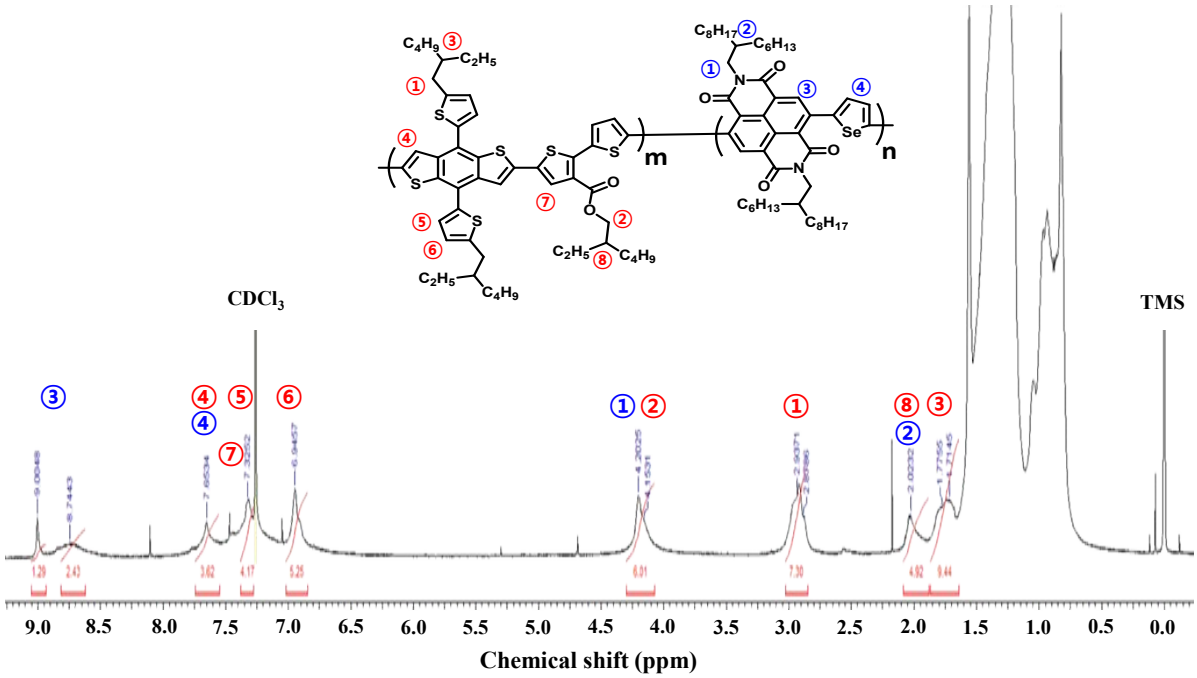

Figure S5. ^{1}H NMR spectrum and assignment of the CDABP.

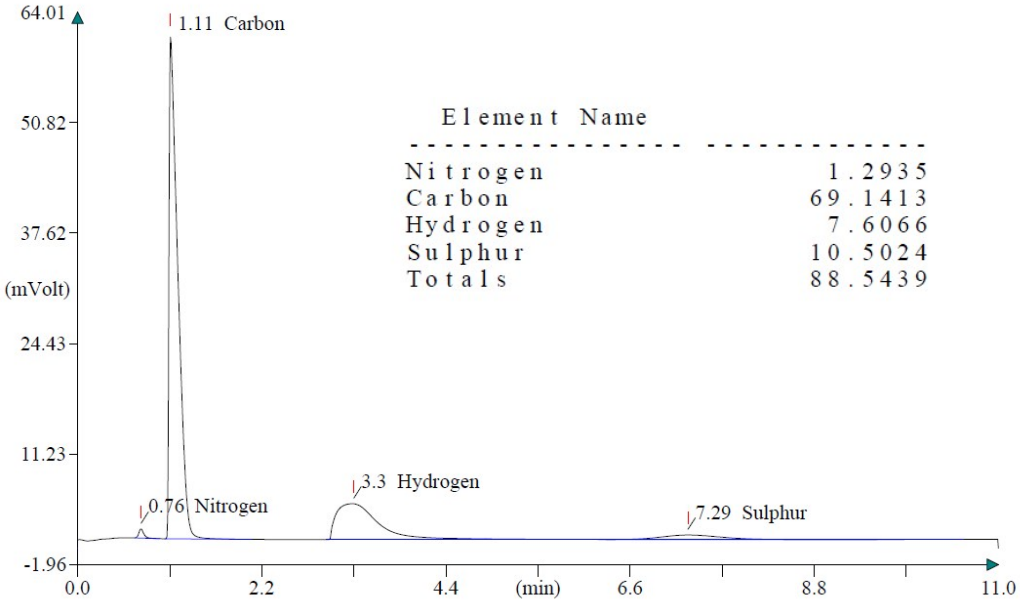

Figure S6. Elemental analysis of the CDABP.

Table S3. A tri-exponential fit to the TRPL signals of **PBDT2T** and **CDABP** in toluene.

Parameter	PBDT2T	CDABP
A_1	0.09	0.18
τ_1 **(ns)**	0.38	0.36
A_2	0.67	0.67
τ_2 **(ns)**	1.2	0.95
A_3	0.24	0.15
τ_3 **(ns)**	2.1	1.9
τ_{avg} **(ns)**	**1.3**	**1.0**

* $S(t) = \sum_{i=1}^{3} A_i \exp(-t/\tau_i)$. The average lifetime was calculated by $\tau_{avg} = \sum_i A_i \tau_i / \sum_i A_i$; The concentration of samples in solution is ~ 10^{-5} M.

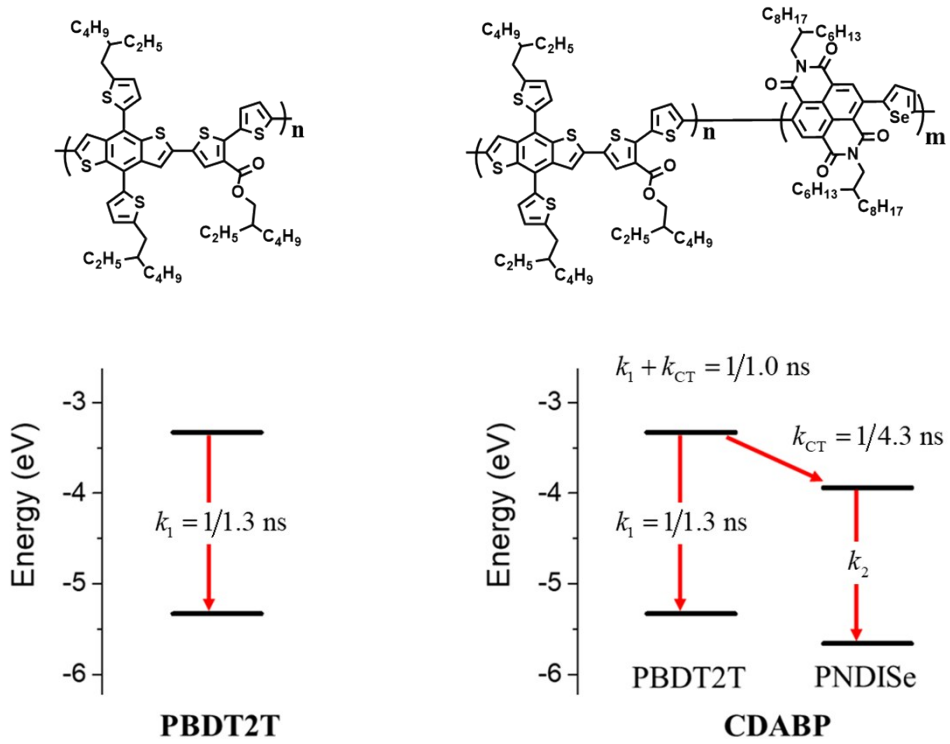

Figure S7. Structures of PBDT2T and CDABP. Energy states in PBDT2T and CDABP.

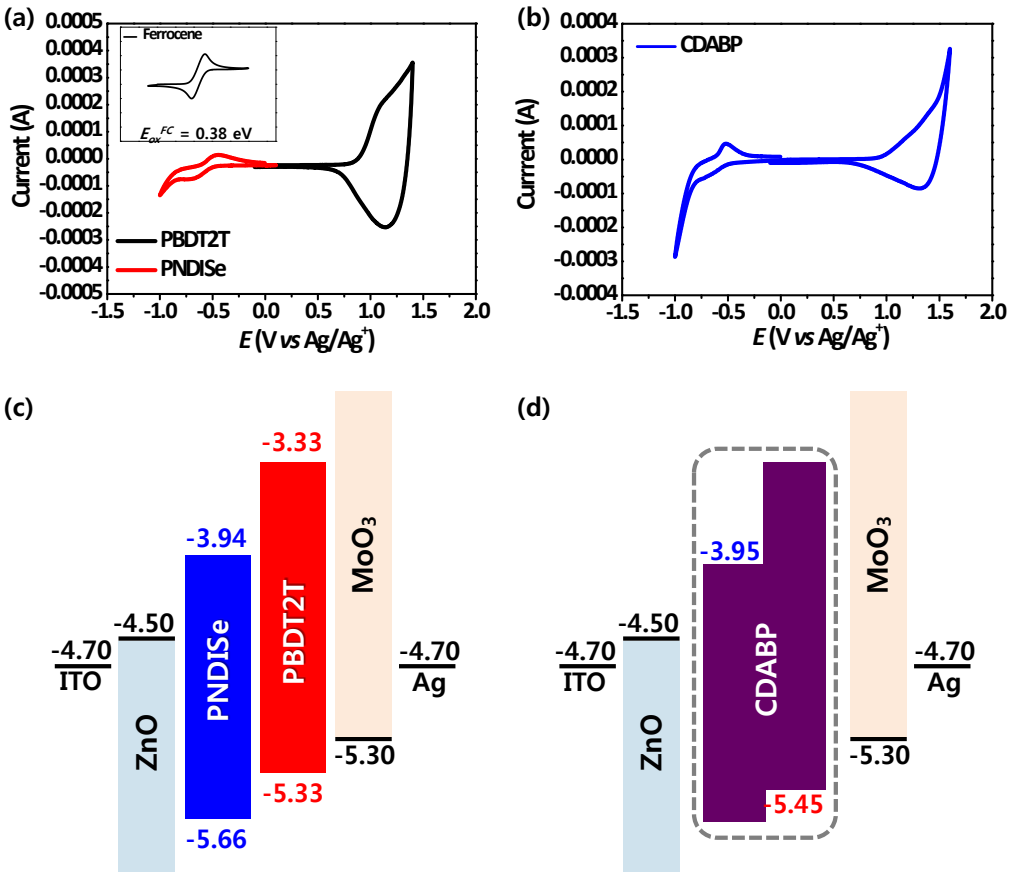

Figure S8. Cyclic voltammograms of PBDT2T, PNDISe (a) and CDABP (b). Energy diagram of all-PSC (c) and CDABP-based SC-PSC device (d).

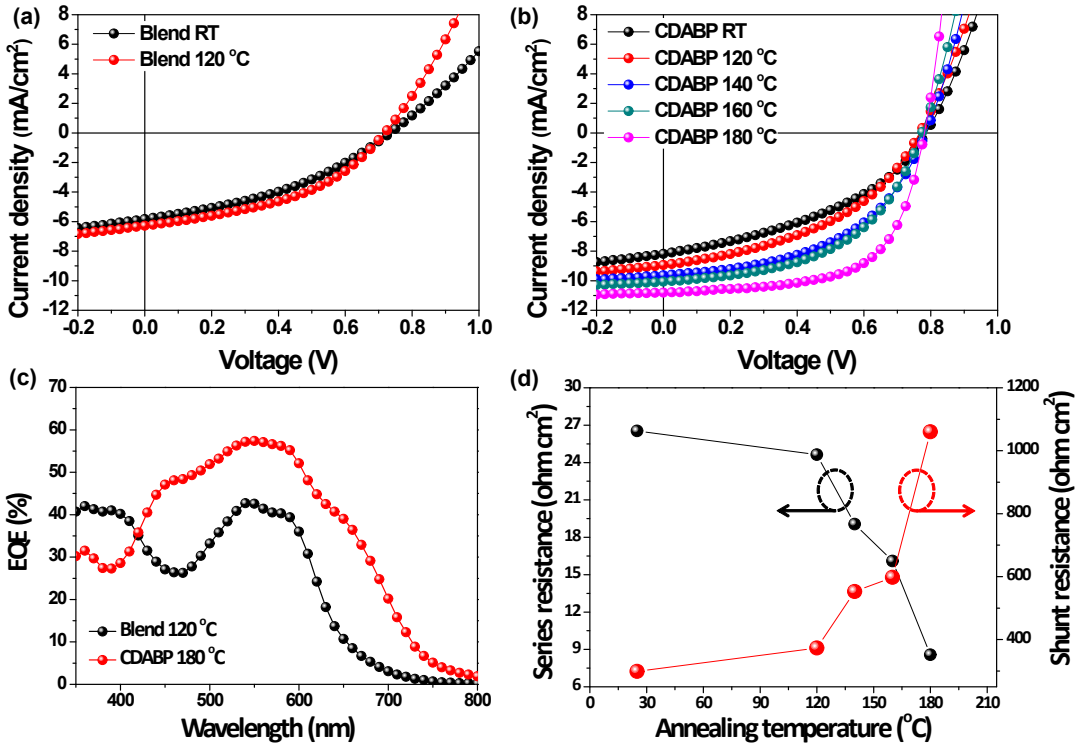

Figure S9. *J-V* characteristics (a,b) and external quantum efficiency (EQE) spectra (c) of blend- and CDABP-based PSCs. Series resistance (R_s) and shunt resistance (R_{sh}) versus annealing temperature of CDABP-based SC-PSCs devices (d).

Table S4. Photovoltaic properties of blend and CDABP made from chlorobenzene solution with a ITO/ZnO/Active layer/MoO_3/Ag device structure measured under AM 1.5G illumination (100 mW cm^{-2}).

Polymer	Annealing Temp. (°C)	V_{oc} (V)	J_{sc} (mA cm^{-2})	*FF* (%)	*PCE* (%)	R_s (Ω cm^2)	R_{sh} (Ω cm^2)
Blend	-	0.73	5.82	37.86	1.62	59.48	303.96
	120 °C 10 min	0.72	6.28	43.04	1.94	37.53	337.55
CDABP	-	0.78	8.15	40.98	2.62	26.54	299.08
	120 °C 10 min	0.77	8.90	43.93	2.99	24.63	373.31
	140 °C 10 min	0.78	9.60	49.74	3.75	19.06	552.95
	160 °C 10 min	0.77	10.02	51.36	3.98	16.09	597.71
	180 °C 10 min	0.78	10.77	62.86	5.28	8.57	1060.00

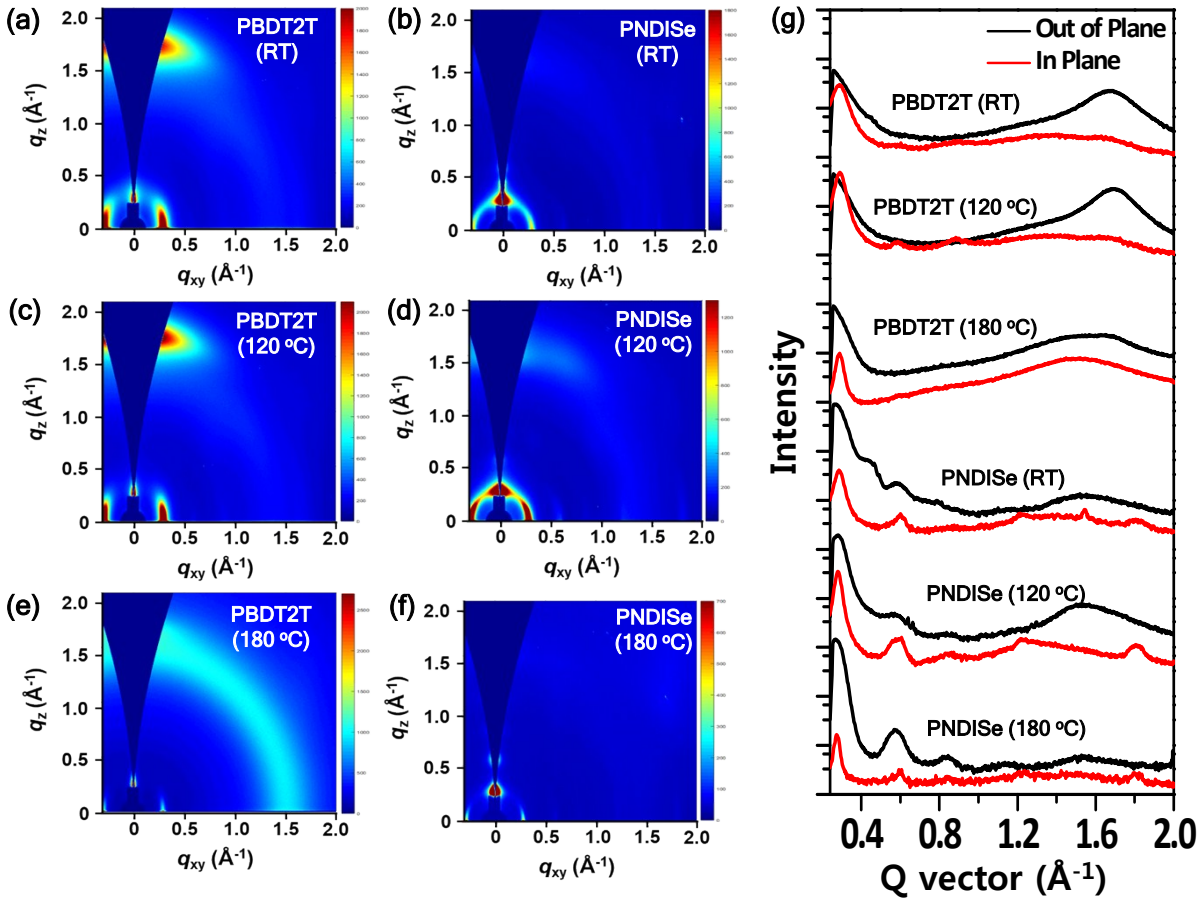

Figure S10. (a-f) 2D GIWAXD patterns of PBDT2T and PNDISe films with the annealing temperature: (g) Out-of-plane and in-plane scattering profiles of the GIWAXD patterns. Annealing time = 10 min.

Table S5. Parameters of out-of-plane and in-plane scattering profiles of PNDISe and PBDT2T films in the GIWAXD patterns

Compound	Out-of-plane				In-plane			
	Temp. (°C)	Direction	q (Å^{-1})	Distance (Å)	Temp. (°C)	Direction	q (Å^{-1})	Distance (Å)
PNDISe	RT	(010)	1.55	4.05	RT	(100)	0.2848	21.66
	RT	(100)	0.26	24.16	RT	(200)	0.60096	10.47
	120	(010)	1.54	4.07	120	(100)	0.28033	22.43
	120	(100)	0.28	22.43	120	(200)	0.60539	10.47
	120	(200)	0.57	11.02	120	(300)	0.84	7.47
	180	(100)	0.27	23.27	180	(100)	0.27362	23.27
	180	(200)	0.57	11.02	180	(200)	0.60538	10.47
	180	(300)	0.84	7.47				
PBDT2T	RT	(010)	1.68	3.73	RT	(100)	0.28929	21.66
	120	(010)	1.68	3.73	120	(100)	0.28927	21.66
	180	(010)	1.68	3.73	120	(200)	0.58767	10.83
					120	(300)	0.88452	7.14
					180	(100)	0.28928	21.66

Table S6. Parameters of out-of-plane and in-plane scattering profiles of CDABP film in the GIWAXD patterns

Compound	Out-of-plane					
	Temp. (°C)	Direction	q ($Å^{-1}$)	Distance (Å)	FWHM (Å)	Coherence Length (Å)
CDABP	RT	(010)	1.66	3.78	0.35404	16.50
	RT	(200)	-	-	-	-
	120	(010)	1.67	3.77	0.29937	19.52
	120	(200)	0.58	10.83	-	-
	180	(010)	1.67	3.77	0.29052	20.11
	180	(200)	0.57	11.02	-	-

Compound	In-plane					
	Temp. (°C)	Direction	q ($Å^{-1}$)	Distance (Å)	FWHM (Å)	Coherence Length (Å)
CDABP	RT	(100)	0.29	21.66	0.05633	103.73
	RT	(200)	0.61	10.30	-	-
	RT	(300)	-	-	-	-
	120	(100)	0.28	22.43	0.0416	140.46
	120	(200)	0.60	10.47	-	-
	120	(300)	0.85	7.39	-	-
	180	(100)	0.28	22.43	0.03045	191.90
	180	(200)	0.61	10.30	-	-
	180	(300)	0.84	7.47	-	-

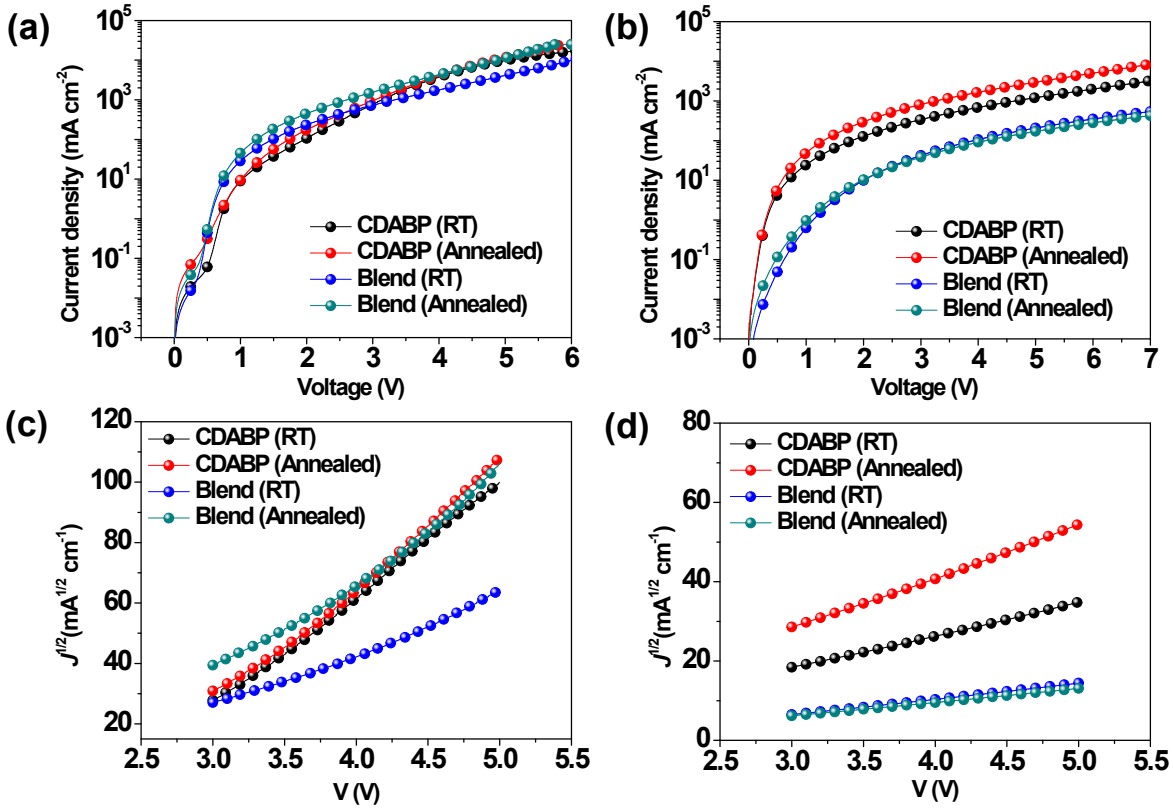

Figure S11. *J-V* curves for hole only device (a) and electron only device (b) of CDABP. SCLC curves for hole mobility (c) and electron mobility (d) of Blend and CDABP.

Table S7. Hole and electron mobility of blend and CDABP films.

Active layer	**Annealing Temp. (°C)**	μ_h (cm^2/Vs)	μ_e (cm^2/Vs)	μ_h/μ_e
CDABP	-	4.50 x 10^{-4}	2.18 x 10^{-5}	20.64
	180	5.08 x 10^{-4}	5.42 x 10^{-5}	9.37
Blend	-	1.08 x 10^{-4}	5.08 x 10^{-6}	21.26
	120	3.51 x 10^{-4}	3.86 x 10^{-6}	90.93

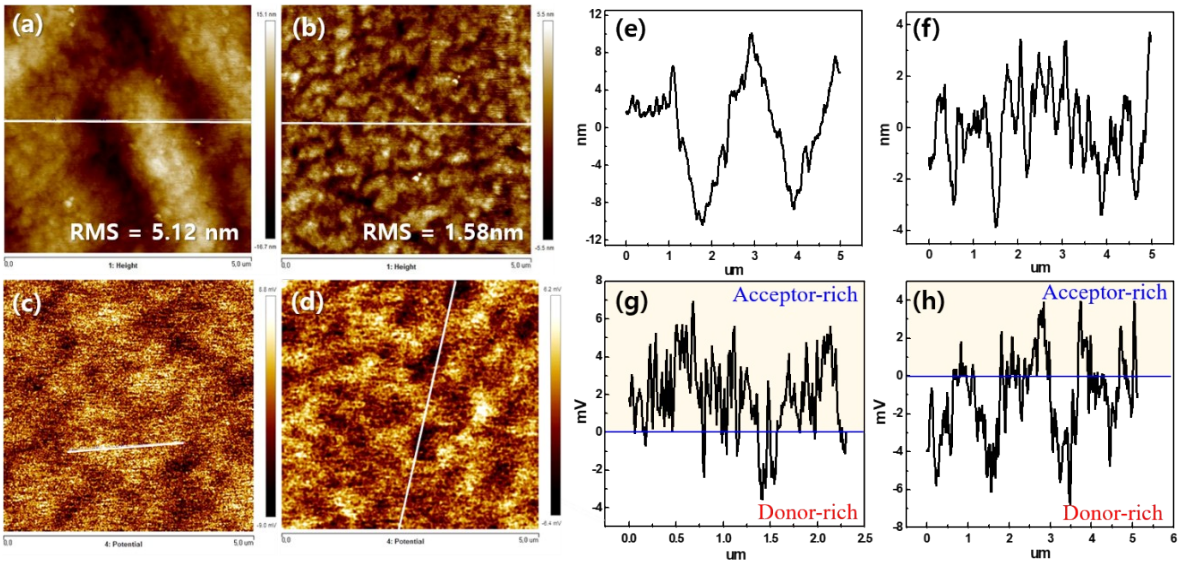

Figure S12. AFM topographic images (a,b) and KPFM potential images (c,d) recorded in the dark. (a,c) As-cast CDABP film, (b,d) annealed CDABP film. Surface profile of: (e) as-cast and (f) annealed film. KPFM potential profile of: (g) as-cast and (h) annealed film. Annealing temperature = 180 °C for 10 min.

Transient absorption (TA) experiments

For TA experiments, the film samples were prepared by spin coating and the absorbance in the visible region was approximately 0.20-0.40 as shown in **Figure S13**. All film samples were excited by a 540 nm pump and subsequently probed by a white light continuum. TA signals measured with PBDT2T and PNDISe films are shown in **Figure S14**. Following excitation by a 540 nm pump pulse, the excitons in both films are generated and may undergo various exciton relaxation processes. In both cases, a fast relaxation occurring at early times results from exciton-exciton annihilation (EEA) and a slow relaxation at long times comes from the exciton relaxation back to the ground state. The fast relaxation at early times in TA signals is accompanied by a gradual spectral shift and gets less significant as the pump intensity is decreased as shown in **Figure S15**. TA signals measured with PBDT2T and

PNDISe films are analyzed by a tri-exponential function as shown in Table S8.

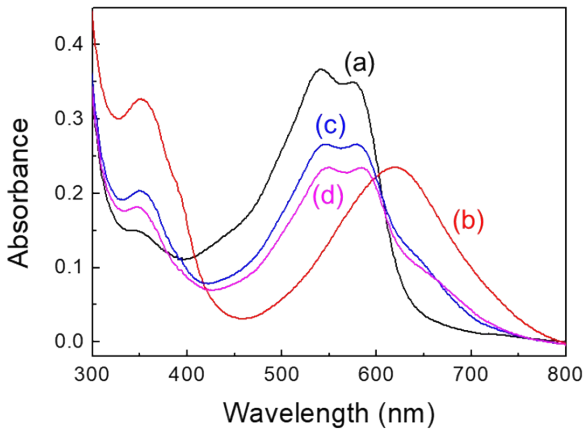

Figure S13. Absorption spectra of (a) PBDT2T, (b) PNDISe, (c) as-cast CDABP and (d) thermally annealed CDABP films used for TA experiments.

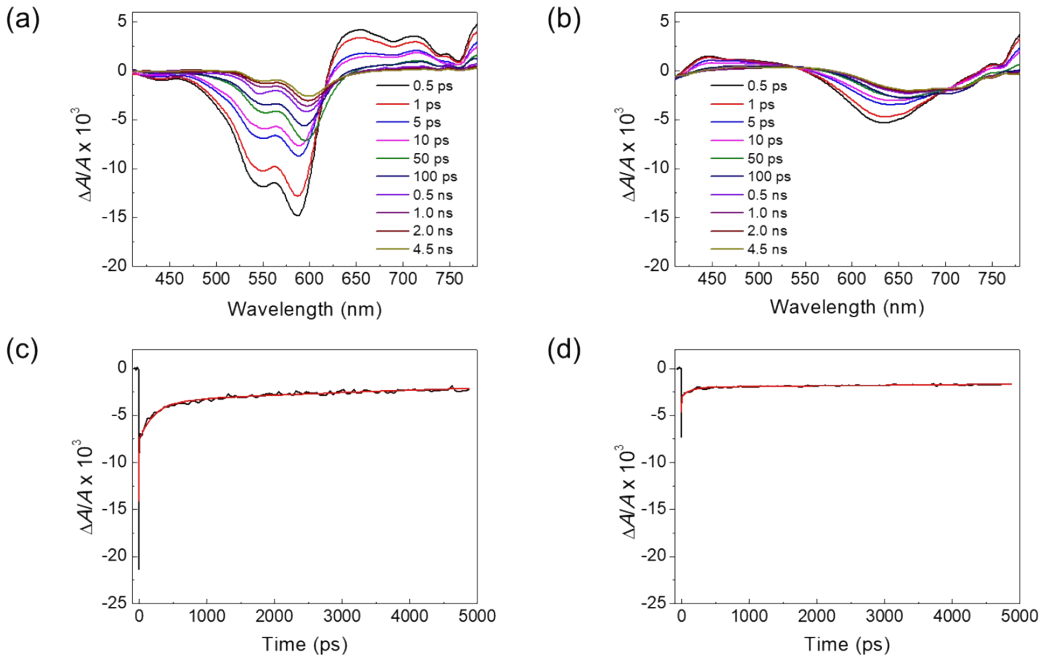

Figure S14. TA signals, $S_{\mathrm{TA}}(t,\lambda_{\mathrm{pr}}) = \Delta A / A$, measured with (a) PBDT2T and (b) PNDISe films as a function of time following excitation at λ_{pu}=540 nm. TA decays of (c) PBDT2T and (d) PNDISe films measured at λ_{pr}=590 and 640 nm, respectively. The red lines are a tri-exponential fit to the TA signals.

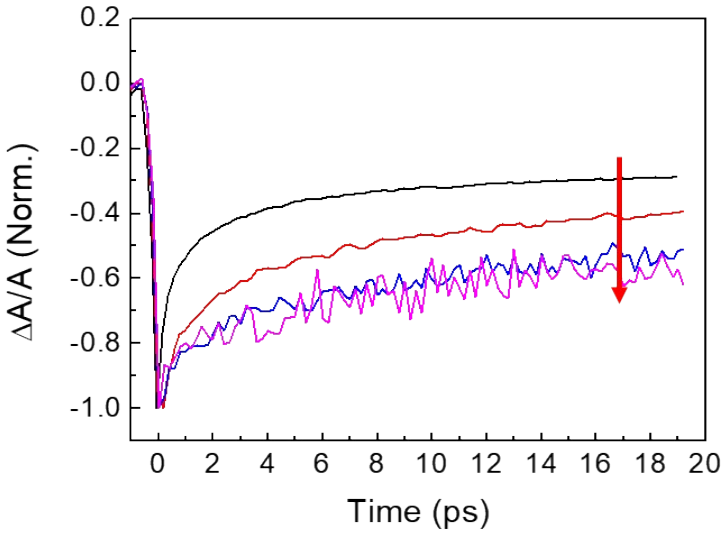

Figure S15. TA signals, $S_{TA}(t, \lambda_{pr} = 590\ \text{nm})$, of PBDT2T film probed at 590 nm as a function of pump intensity (λ_{pu} = 540 nm). The pump intensity is decreased as indicated by the arrow. The fast component in the TA decays is significantly reduced as the pump intensity is reduced. This indicates that exciton-exciton annihilation (EEA) at early times gets less significant as the number of generating excitons is reduced.

Table S8. Analysis of TA signals, $S_{TA}(t, \lambda_{pr})$, of PBDT2T and PNDISe films by a tri-exponential fit

Parameter	**PBDT2T (λ_{pr} = 590 nm)**	**PNDISe (λ_{pr} = 640 nm)**
A_1	0.52	0.41
τ_1	2.3 ps	3.3 ps
A_2	0.26	0.20
τ_2	0.22 ns	0.12 ns
A_3	0.22	0.39
τ_3	9.7 ns	26 ns

$S_{TA}(t, \lambda_{pr}) = \sum_{i=1}^{3} A_i \exp(-t / \tau_i)$

Table S9. Analysis of TA signals, $S_{TA}(t,\lambda_{pr})$, measured at λ_{pr} = 710 nm by a multi-exponential fit.

Parameter	As-cast CDABP film	Annealed CDABP film
A_1	-0.19±0.04	-0.034±0.005
τ_1	13±3 ps	6.5±1.8 ps
A_2	0.18±0.03	0.056±0.004
τ_2	23±2 ps	33±4 ps
A_3	0.056±0.001	0.046±0.001
τ_3	0.83±0.04 ns	0.74±0.04 ns
A_4	0.30±0.03	0.19±0.02
τ_4	39±10 ns	53±3 ns

$S_{TA}(t,\lambda_{pr}) = \sum_{i=1}^{4} A_i \exp(-t/\tau_i)$

Additional References

S1. S. M. Lindner, S. Hüttner, A. Chiche, M. Thelakkat, G. Kraush, *Angew. Chem., Int. Ed*. **2006**, *45*, 3364.

S2. L. Bu, X. Guo, B. Yu, Y. Qu, Z. Xie, D. Yan, Y. Geng, F. Wang, *J. Am. Chem. Soc.* **2009**, *131*, 13242.

S3. L. Bu, X. Guo, B. Yu, Y. Fu, Y. Qu, Z. Xie, D. Yan, Y. Geng, F. Wang, *Polymer*. **2011**, *52*, 4253.

S4. S. Koyuncu, H.-W. Wang, F. Liu, K. Bugra Toga, W. Gu, T. P. Russell, *J. Mater. Chem. A*. **2014**, *2*, 2993.

S5. J. Qu, B. Gao, H. Tian, X. Zhang, Y. Wang, Z. Xie, H. Wang, Y. Geng, F. Wang, *J. Mater. Chem. A*. **2014**, *2*, 3632.

S6. F. Di Maria, M. Biasiucci, F. Paolo Di Nicola, E. Fabiano, A. Zanelli, M. Gazzano, E. Salatelli, M. Lanzi, F. Della Sala, G. Gigli, G. Barbarella, *J. Phys. Chem. C*. **2015**, *119*, 27200.

S7. Y. Li, K. Shetye, K. Baral, L. Jin, J. D. Oster, D.-M. Zhu, Z. Peng, *RSC Adv.* **2016**, *6*, 29909.

S8. D. H. Lee, J. H. Lee, H. J. Kim, S. Choi, G. E. Park, M. J. Cho, D. H. Choi, *J. Mater. Chem. A*. **2017**, *5*, 9745.

S9. J. H. Lee, A. Kim, H. J. Kim, Y. Kim, S. Park, M. J. Cho, D. H. Choi, *ACS Appl. Mater. Interfaces.* **2018**, *10*, 18974.

S10. G. G. Malliaras, J. R. Salem, P. J. Brock, C. Scott, *Phys. Rev. B,* **1998**, *58*, 13411.